Optics Communications 286 (2013) 363–367

Contents lists available at SciVerse ScienceDirect

Optics Communications

journal homepage: www.elsevier.com/locate/optcom

A spectral analysis of an integrated photomixer/antenna in a homodyne terahertz photomixing system

Han-Cheol Ryu [a,*], Seong-Ook Park [b], Kwang-Yong Kang [a]

[a] Electronics and Telecommunications Research Institute, 218 Gajeongno, Yuseong-Gu, Daejeon 305-700, Korea
[b] Korea Advanced Institute of Science and Technology, 291 Daehakno, Yuseong-Gu, Daejeon 305-701, Korea

ARTICLE INFO

Article history:
Received 27 June 2012
Received in revised form
3 September 2012
Accepted 6 September 2012
Available online 18 September 2012

Keywords:
Integrated photomixer/antenna
Terahertz photomixing
Impedance mismatch factor
Friis power transmission formula
Propagation loss

ABSTRACT

An analysis has been carried out to estimate the spectral characteristics of an integrated photomixer/antenna in a homodyne photomixing system. The analysis adopts the impedance mismatch factor and Friis power transmission formula used in communication links based on the conventional analysis theory of a terahertz photomixer. The analysis and experimental results have proved that an impedance matching condition between the impedance of a photomixer and the input impedance of an antenna is directly related with photomixing terahertz wave generation. The Friis formula is introduced to calculate the propagation loss of the wave from a transmitter to a receiver in a homodyne photomixing system. A log-periodic antenna was used to ensure a high dynamic range in a broad frequency region. The dynamic range of the homodyne terahertz photomixing system was about 60 dB near 100 GHz and decreased with an increasing frequency from 10 GHz to 1000 GHz. The measured results agree well with the theoretically analyzed results and prove that the terahertz photomixing power is closely related to impedance mismatch factor and it could be estimated in the homodyne terahertz photomixing system without a terahertz power detector.

1. Introduction

Homodyne terahertz systems have received a considerable amount of attention as an important candidate for terahertz spectroscopy, sensing and imaging systems [1–3]. A continuous-wave (CW) terahertz photomixing system is superior to a pulsed terahertz system for industrialization because of the low cost and the small size. It offers the advantages of frequency selectivity and a much higher frequency resolution that enables real-time measurements in the frequency domain [4,5]. A photoconductive photomixer was used to generate the CW in the terahertz frequency region by using two CW laser beams possessing different frequencies. The most important duty of a CW terahertz photomixing system is to increase the output power of an integrated photomixer/antenna. Improvements to a terahertz output power have been achieved through many efforts to optimize a photomixer and antenna geometry and in the development of the photomixer substrate material [6–8]. The achieved power is still insufficient for real applications; the desired power improvement now needs to be conducted by optimizing the photomixer and antenna design. In order to achieve the optimization of the design, the theoretical analysis model of an integrated photomixer/antenna is very important. Most of the studies on the theoretical analysis have been devoted to the concept of the photomixer acting as a discrete current source connected to an antenna without consideration of impedance matching between photomixer and antenna [9,10]. However, improvement of the impedance matching by using a resonant antenna can increase the output power of an integrated photomxier/antenna [11,12]. Impedance matching needs to be added to the theoretical analysis in order to estimate the power more accurately. A homodyne terahertz photomixing system is appropriate for the verification of the analysis used to characterize an antenna because the frequency characteristics of an antenna in a CW system are not affected by an optical excitation, whereas the characteristics of an antenna in a pulsed system are significantly influenced by an optical pulse shape [13]. When a terahertz wave propagates from a transmitter to a receiver in a homodyne system, a propagation loss varies according to the frequency. Therefore the spectral analysis of an antenna by using a homodyne system should consider a propagation loss as a function of the frequency.

In this paper, the theoretical analysis of an integrated photomixer/antenna in a homodyne terahertz system in the frequency domain is presented. The analysis method combines the effects of an impedance matching between photomixer and antenna based on the conventional analysis theory of a terahertz photomixer for the calculation of the generated terahertz power in a transmitter. Furthermore, the analysis includes the Friss power transmission

* Corresponding author.: Tel: +82 42 860 5650; fax: +82 42 860 4802
E-mail address: hcryoo@etri.re.kr (H.-C. Ryu).

0030-4018/$ - see front matter © 2012 Elsevier B.V. All rights reserved.
http://dx.doi.org/10.1016/j.optcom.2012.09.021

formula used in a communication link in order to estimate the received terahertz power in a receiver after wave propagation from a transmitter. There are four necessary factors needed to analyze an integrated photomixer/antenna; the input resistance of an antenna, the capacitance of a photomixer, the reflection coefficient between photomxier and antenna, and the photocarrier lifetime of a substrate material. In order to achieve a high dynamic range in a broad frequency region, a log-periodic antenna having a self-complementary property was used [14,15]. The input resistance of a log-periodic antenna and the capacitance of an interdigitated photomixer were calculated by using an electromagnetic (EM) simulator. The reflection coefficient (Γ) between photomixer and antenna was also calculated by using the EM simulator; the port impedance of an antenna was renormalized to 100 kΩ because the measured resistance of a photomixer was about 100 kΩ when the photomixer was excited by a light. The photocarrier lifetime was measured using time-resolved reflectance measurements. In order to verify the accuracy of the proposed analysis, the calculated results were compared to the measured ones in the homodyne terahertz photomixing system composed of an all-fiber path for a laser beam.

2. Photomixing theory and data analysis

Fig. 1 shows an equivalent circuit diagram of an integrated photomixer/antenna. A photomixing process occurs by illuminating a photomixer fabricated on the photoconductor with two CW laser beams. These lasers have slightly different frequencies, v_1 and v_2, and powers, P_1 and P_2, and are collinear in space and linearly polarized. The photocurrent $i(\omega,t)$ is modulated only at the difference frequency of the lasers because the time period of two lasers is much shorter than the photocarrier life-time of the photoconductor. The capacitance $C(\omega)$ represents charge accumulating effects in the interdigitated photomixer. The bias voltage V_B can be modulated at several kHz for the THz signal detection by using lock-in detection techniques. The time-dependent conductance, $G(\omega,t)$ is obtained from the carrier density generated in the photoconductive gap.

The instantaneous power incident on a photomixer is taken from [16]:

$$P(\omega,t)=P_1+P_2+2\sqrt{mP_1P_2}\cos(\omega,t) \tag{1}$$

where $\omega=2\pi(v_1-v_2)$, and m is the mixing efficiency that varies between 0 and 1 depending on the spatial overlap of two lasers [3]. The photocarrier density in the photoconductive gap of a photomixer is the solution of the Eq. (2).

$$\frac{dn}{dt}=\frac{\eta}{h\nu Ad}P(\omega,t)-\frac{n}{\tau} \tag{2}$$

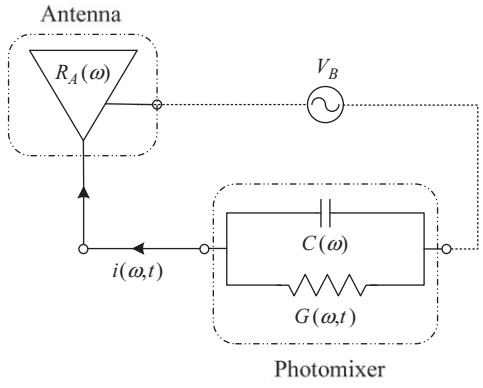

Fig. 1. Equivalent circuit diagram of an integrated photomixer/antenna.

where n is the instantaneous photocarrier pair density, η is the quantum efficiency (the number of photocarrier pairs per incident photon), A is the active area, d is the absorption depth, and $h\nu$ is the mean photon energy. The second term in Eq. (2) indicates the exponential decay of carriers with a $1/e$ decay lifetime characterized by τ. Using the equivalent circuit from Fig. 1, the instantaneous power dissipated in an antenna resistance can be written as:

$$P_A(\omega,t)=R_A(\omega)\left[\frac{V_B}{R_A(\omega)+[G(\omega,t)+j\omega C(\omega)]^{-1}}\right]^2 \tag{3}$$

The terahertz power in an antenna is determined finally in (4) by disregarding the constant offset and averaging the powers varying with time, and adding the impedance matching condition between the output impedance of a photomixer and the input impedance of an antenna.

$$P_{A\_THz}(\omega)=\eta_c(1-|\Gamma|^2)\frac{R_A(\omega)\tau^2}{\left(1+(\omega\tau)^2\right)\left(1+(\omega R_A(\omega)C(\omega))^2\right)} \tag{4}$$

where η_c is defined as the total optical-to-electrical conversion efficiency related with the incident power, the quantum and mixing efficiency, the bias voltage, the mobility of the photoconductor, and the geometry of a photomixer. Γ is the reflection coefficient between photomixer and antenna, that is defined as $(Z_{ant}\text{-}Z_{mixer})/(Z_{ant}+Z_{mixer})$, where Z_{ant} is the input impedance of an antenna and Z_{mixer} is the output impedance of a photomixer. The impedance mismatch factor $(1\text{-}|\Gamma|^2)$ represents the fraction of power delivered to an antenna from a photomixer based on the ratio of the impedance of a photomixer and an antenna. Eq. (4) shows that the radiated terahertz output power is closely related to the photocarrier lifetime and the capacitance of a photomixer, and especially related to an antenna impedance.

For data analysis, a homodyne terahertz photomixing system is considered to be a simple communication link having same transmitting and receiving antennas in order to calculate power transfer. The power transmission formula in the communication link is:

$$P_r=P_t\frac{G_tG_r\lambda^2}{(4\pi R)^2} \tag{5}$$

In our system, P_r and P_t are interpreted as the received power at a receiving antenna and the transmitted power by a transmitting antenna, respectively. The gains of transmitting and receiving antennas, G_t and G_r are set to be constant in the frequency domain because the absolute value of the power is outside the scope of this study. The received power in our system can be expressed as:

$$P_{r\_THz}(\omega)\propto(1-|\Gamma|^2)\frac{R_A(\omega)\tau^2}{\omega^2\left(1+(\omega\tau)^2\right)\left(1+(\omega R_A(\omega)C(\omega))^2\right)} \tag{6}$$

The photocurrent $I_{ph}(\omega)$ obtained by using the lock-in amplifier in our system and the received power $P_{r\_THz}(\omega)$ are related by $P_{r\_THz}(\omega)\propto I_{ph}^2(\omega)$, that is, the square of the measured photocurrent is proportional to the received terahertz power.

3. Experimental setup

A homodyne system setup is shown schematically in Fig. 2. Our system is composed of an all-fiber path for laser beams in order to increase the flexibility and power stability. Two distributed-feedback tunable diode lasers, operating at around 853 and 855 nm, respectively, are coupled into a 2×4 fiber array made of single mode, polarization-maintaining fiber. Approximately 1% of each guided laser's power is extracted from the 2×4 fiber combiner/splitter to provide feedback control for the lasers. This feedback control system can eliminate frequency fluctuations

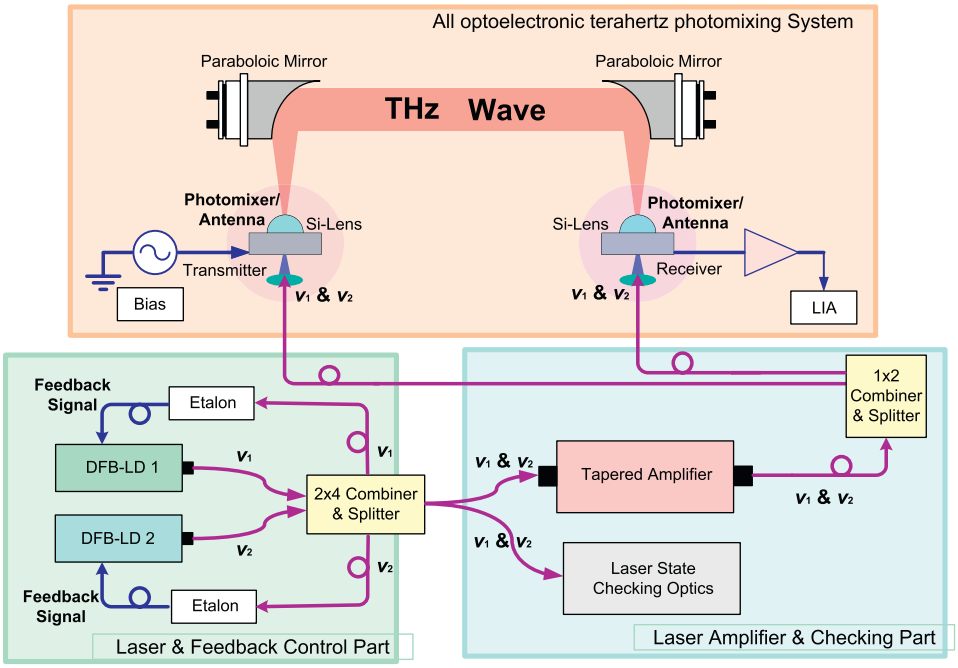

Fig. 2. Homodyne terahertz photomixing system setup.

due to thermal drift or electronic noise. The frequency of the laser can be controlled on the MHz level by the feedback system. Additionally, the laser current is regulated based on the feedback laser power to maintain a constant average laser output power. One of superimposed laser beams from the combiner/splitter is fed into a tapered semiconductor amplifier, the other one is used for checking the frequency and power of two lasers. The amplifier amplifies two laser beams while maintaining spectral properties, such as the linewidth and the tunability. The output power of the amplifier is coupled to a fiber-optical 50:50 splitter and divided into two fiber outputs having the beat signal with the same power. The two outputs are connected to two integrated photomixer/antennas to play the role of terahertz transmitter and receiver, respectively, in a homodyne terahertz photomixing system.

A photoconductive 1.5 μm GaAs layer was grown on 350 μm semi-insulating (SI)-GaAs using a molecular-beam epitaxy (MBE) system at a temperature of 275 °C for a photomixer/antenna. After growing, it was annealed in situ at a temperature of 600 °C for 10 min in ambient As_4. The photocarrier lifetime of the low-temperature-grown (LTG)-GaAs was measured using time-resolved reflectance measurements employing a femtosecond self-mode-locked Ti:sapphire laser tuned to $\lambda = 790$ nm in order to calculate a terahertz output power. The measured photocarrier lifetime was 1 ps, as shown in Fig. 3.

For the THz emission and detection a log-periodic antenna and an interdigitated photomixer were fabricated on the LTG-GaAs using photolithography and electron-beam lithography, respectively. The log-periodic broadband antenna was adopted in order to extract the frequency characteristics of an antenna operating in a homodyne terahertz photomixing system in a wide frequency range. The shape of an interdigitated capacitor (IDC) was used for a photomixer to increase the optical-to-electrical conversion efficiency. The dimensions of the IDC are: the total number of fingers = 2, the overlap length = 4.6 μm, the finger width = 0.3 μm, and the gap = 1.7 μm. The photomxier is integrated into the feed point of a log-periodic antenna as the source for an antenna. The photocurrent in a transmitter chip is generated when the photocarriers excited by two DFB-LDs are accelerated by a bias voltage.

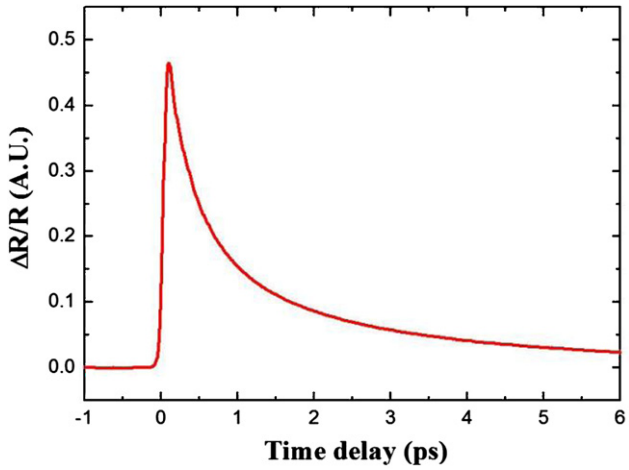

Fig. 3. Time-resolved reflectance measurements of LTG-GaAs.

The generated photocurrent in a photomixer is coupled to an antenna and radiated into free space via an attached silicon lens. The transmitted terahertz wave from a transmitter chip is collimated and focused onto a receiver chip through two off-axis parabolic mirrors in a homodyne terahertz photomixing system, as seen in Fig. 2. A receiver operates in a similar way to a transmitter, but the terahertz wave incident on a receiver plays the role of a bias voltage in a transmitter chip. A voltage proportional to the received electric field induces the photocurrent by accelerating the photocarriers excited in a receiver chip.

4. Results and discussions

In order to verify the theoretical analysis, the input resistance of a log-periodic antenna and the capacitance of an interdigitated photomixer were calculated by using the CST microwave studio (MWS) EM simulator. Fig. 4 shows the simulated input resistance of the antenna and capacitance of a photomixer. As shown in Fig. 4(a), there are several peaks under 300 GHz and one peak

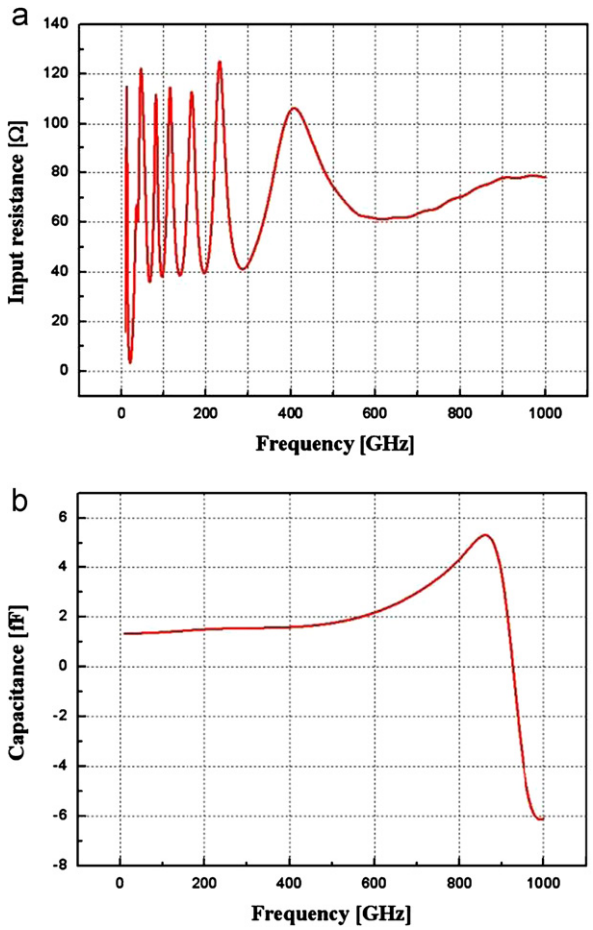

Fig. 4. Simulated results: (a) the input resistance of a log-periodic antenna and (b) the capacitance of an interdigitated photomixer.

near 400 GHz because of the resonance characteristics of the several teeth found in the log-periodic antenna. In Fig. 4(b), the interdigitated photomixer shows an inductive behavior over 930 GHz. The inductive behavior of the photomixer is out of the scope of this analysis, but the optimization of the inductive behavior of the photomixer with the reactance of an antenna could increase the radiation efficiency of an integrated photomixer/antenna in the terahertz region.

The reflection coefficient (Γ) between photomixer and antenna was calculated using the EM simulator; the port impedance of an antenna was renormalized to 100 kΩ because the measured resistance of a photomixer was about 100 kΩ when the photomixer was excited by the lasers. The reflection coefficient and the impedance mismatch factor ($1-|\Gamma|^2$) seen in Fig. 5 show that the fraction of power delivered to an antenna from a photomixer is between approximately 0.001 and 0.005.

Most of the generated power in a photomixer is reflected because of the impedance mismatch between the output impedance of a photomixer and the input impedance of an antenna. This impedance mismatch factor could be ameliorated by using resonant antennas having a high input impedance in the specific frequency range.

The received power was calculated with the measured photocarrier lifetime and the calculated antenna impedance and photomixer capacitance found in Figs.4 and 5 using (6). The theoretically calculated results are compared in Fig. 6 to the measured results in order to verify the proposed analysis. The inset shows the SNR in the lower frequency region. For the comparison, the photocurrent of the system was measured using lock-in detection techniques. The bias of

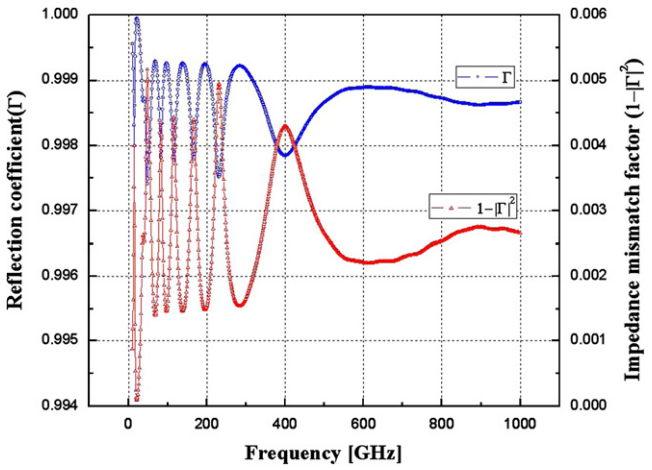

Fig. 5. Simulated reflection coefficient and impedance mismatch factor.

a transmitting photomixer/antenna was modulated at a frequency of 3 kHz and a maximum voltage of 15 V. The lock-in time constant was set to 300 ms. Each photomixer/antenna was excited by an optical power of 30 mW. The noise photocurrent was measured by blocking the terahertz beam in order to determine the SNR of the system. The difference frequency was varied from 10 GHz to 1000 GHz in steps of 100 MHz.

The amplitude of a detected photocurrent is proportional to the amplitude of a terahertz electric field. The phase of a photocurrent oscillates with the difference between an optical path traveled by a laser beat to the receiver and an optical path of a laser beat to a transmitter plus a terahertz path from a transmitter to a receiver. There are two different kinds of methods to control the phase difference. In the first method, the phase difference can be controlled simply by changing an optical or a terahertz path. In this case, for each frequency, the phase of an optical path to a receiver and an optical path to a transmitter plus a terahertz path needs to be equalized by changing an optical or terahertz path to maximize the photocurrent at that frequency. Alternatively, the phase difference also can be adjusted by scanning an optical beat frequency. The maxima of the oscillating photocurrent are equally spaced in frequency. In this study, the difference frequency was scanned without using a delay line and so the oscillating photocurrent according to a frequency was measured. The values of the photocurrent at the equally spaced maxima were used to determine the SNR of the measured photocurrent. The SNR of the measured power was about 60 dB near 100 GHz and the water vapor absorption line appeared at 558 and 753 GHz. The calculated powers were scaled to the measured value at the peak of nearly 166 GHz in order to compare the calculated results to the measured one. Fig. 6 clearly shows the effects of the impedance mismatch factor and the Friss power transmission formula. The red line shows the calculated power considering both the impedance mismatch factor and the power transmission formula. The blue line and the purple line show the calculated power considering only the Friss formula and only the impedance mismatch factor, respectively. The calculated power without consideration of the impedance mismatch factor, i.e. the blue line, shows discrepancies in the ripple size under 300 GHz and the amplitude levels over 500 GHz. The gap between the measured power and the calculated power, not considering the Friss formula, increases monotonically with an increasing frequency. These results imply that the generated power in an integrated photomixer/antenna can be roughly estimated from the results measured in a homodyne terahertz system by removing a propagation loss as a function of the frequency. The peaks in

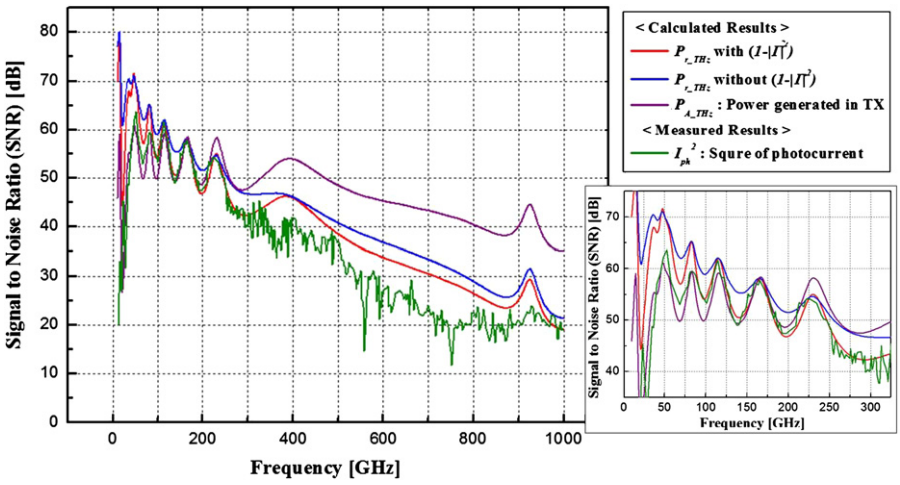

Fig. 6. Comparison of the signal to noise ratio (SNR) between the calculated and measured results. Inset shows the SNR in the lower frequency region.

the calculated results between 900 and 1000 GHz are attributed to the change of IDT photomixer characteristics from a capacitor to an inductor. The calculated data over the frequency at which the characteristics of an IDT photomixer are changed to inductor is not correct because the effect of the inductor is not analyzed in this paper. The SNR of the calculated results are higher than the SNR of the measured one under 100 GHz because the terahertz path is not sufficient to satisfy the Friss formula in that frequency region and the gain of the silicon lens under 100 GHz is less than that of silicon lens over 100 GHz. The small discrepancies over 300 GHz are due to the misalignment between the transmitter and receiver and the attenuation that occurs during the propagation of the wave from the transmitter to the receiver through the two parabolic mirrors and air. The measured results generally agree well with the calculated results by the proposed analysis including the impedance mismatch factor and the Friss power transmission formula. The terahertz photomixing power is closely related to impedance mismatch factor and it could be estimated in a homodyne terahertz photomixing system without a terahertz power detector. And the power could be improved by optimizing the effects of the impedance mismatch factor.

5. Conclusions

This paper has presented a spectral analysis method for an integrated photomixer/antenna in a homodyne terahertz photomixing system. The analysis includes the impedance mismatch factor and the Friis power transmission formula based on the conventional analysis theory of a terahertz photomixer. A photomixer/antenna has been characterized over the frequency region of 10–1000 GHz. The SNR of the measured power was approximately 60 dB near 100 GHz and decreased monotonically with an increasing frequency. The calculated results using the analysis method agree well with the measured one. The measured results prove that the terahertz photomixing power is closely related to impedance mismatch factor and it could be estimated in the homodyne terahertz photomixing system without a terahertz power detector.

Acknowledgments

This work was supported by the IT R&D program of MKE/KEIT, Rep. of Korea 2006-S-005-4, Development of THz-wave oscillation/modulation/detection module and signal sources technology

References

[1] M. Tonouchi, Nature Photonics 1 (2007) 97.
[2] D. Grischkowsky, S. Keiding, M.V. Exter, C. Fattinger, Journal of the Optical Society of America B 7 (1990) 2006.
[3] B. Sartorius, H. Roehle, H. Kunzel, J. Bottcher, M. Schlak, D. Stanze, H. Venghaus, M. Schell, Optics express 16 (2008) 9565.
[4] S. Verghese, K.A. McIntosh, S. Calawa, W.F. Dinatale, E.K. Duerr, K.A. Molvar, Applied Physics Letters 73 (1998) 3824.
[5] K.J. Siebert, H. Quast, R. Leonhardt, T. Loffer, M. Thomson, T. Bauer, H.G. Roskos, S. Czasch, Applied Physics Letters 80 (2002) 3003.
[6] F. Nakajima, T. Furuta, H. Ito, Electronics Letters 40 (2004) 20.
[7] E.A. Michael, B. Vowinkel, R. Schieder, M. Mikulics, M. Marso, P. Kordos, Applied Physics Letters 86 (2005) 111120.
[8] I.C. Mayorga, E.A. Michael, A. Schmitz, P. Wal, R. Gusten, K. Maier, A. Dewald, Applied Physics Letters 91 (2007) 031107.
[9] E.R. Brown, F.W. Smith, K.A. McIntosh, Journal of Applied Physics 73 (1993) 1480.
[10] K.A. McIntosh, E.R. Brown, K.B. Nichols, O.B. McMahon, W.F. DiNatale, T.M. Lyszczarz, Applied Physics Letters 67 (1995) 3844.
[11] S.M. Duffy, S. Verghese, K.A. McIntosh, A. Jackson, A.C. Gossard, S. Matsuura, IEEE Transactions on Microwave Theory and Techniques 49 (2001) 1032.
[12] I. Woo, T.K. Nguyen, H. Han, H. Lim, I. Park, Optics Express 18 (2010) 18532.
[13] S. Matsuura, M. Tani, K. Sakai, Applied Physics Letters 70 (1997) 559.
[14] R. Mendis, C. Sydlo, M. Feiginov, P. Meissner, H.L. Hartnagel, IEEE Antennas and Wireless Propagation Letters 4 (2005) 85.
[15] R. Singh, C. Rockstuhl, C. Menzel, T.P. Meyrath, M. He, H. Giessen, F. Lederer, W. Zhang, Optics Express 17 (2009) 9971.
[16] I.S. Gregory, C. Baker, W.R. Tribe, I.V. Bradley, M.J. Evans, E.H. Linfield, A.G. Davies, M. Missous, IEEE Journal of Quantum Electronics 41 (2005) 717.